ESI

for

A self-stabilized amphiphilic fluorescent sensor enables the ratiometric detection of human serum albumin in urine

Mingwei Yan [a, ‡], Immanuel David Charles [a, ‡], and Bin Liu [a, *]

[a] College of Material Science and Engineering, Guangdong Provincial Key Laboratory of New Energy Materials Service Safety, Shenzhen University, Shenzhen 518060, PR China.

‡ These authors contributed equally to this work.

*Corresponding author:

Bin Liu, bliu@szu.edu.cn

1. Materials and instruments

1.1 Materials

All chemicals warfarin, amlodipine, budesonide, chloral hydrate, chlorpropamide, digitoxin, phenytoin, potassium hydroxide (KOH), cesium carbonate (Cs2CO3) and solvents dichloromethane (DCM), toluene, ethyl acetate (EA), dimethyl sulfoxide (DMSO), acetonitrile (ACN), methanol (MeOH), ethanol (EtOH), N,N-dimethylformamide (DMF), dimethyl sulfoxide-d_6 (DMSO-d_6), 30% hydrogen peroxide solution (H_2O_2) and $NaHCO_3$ solution were purchased from Shanghai Bide Pharmatech Co.Ltd, Shanghai Aladdin BioChem Technology Co.Ltd, and Shenzhen Changtai Chemical Technology Co.Ltd without further purification. All biological analytes including human serum albumin (HSA), Na^+, Cl^-, Ca^{2+}, SO_4^{2-}, K^+, NO_3^-, glutathione (GSH), glutamic acid (Glu), proline (Pro), cysteine (Cys), arginine (Arg), tryptophan (Trp), carbolic anhydrase, lysozyme, urine acid (UA), urea, creatinine (Cre), cortisol, glucose, lactose (Lac), trypsin, proteinase were purchased from Sigma-Aldrich Co.Ltd without further purification. Phosphate buffered saline (PBS, 100 mM, pH 7.4) was purchased from J&K scientific. The urine sample was obtained from healthy individual (Mingwei Yan).

1.2 Instruments

^1H NMR and ^{13}C NMR spectra were both measured by a Bruker AVANCE III 500-MHz spectrometer. HRMS was measured on a Thermo Fisher Q Exactive spectrometer. UV–Vis absorption and fluorescence spectra were tested by a Thermo-Fisher Evolution 220 and Thermo-Fisher Lumina fluorometer, respectively. Fluorescence lifetimes were obtained by Horiba DeltaFlex with 453 nm Laser NanoLED. DLS datas were collected by using Malvern's ZETASIZER NANO ZSP instrument.

2. Methods

2.1 Photophysical experiments

The PBS buffer (1 mM, pH 7.4) was 100-time diluted from a stock PBS buffer before preparing the stock solution of HSA (0.5 mM). The stock solution of DCTB was prepared in DMSO with concentration of 10 mM. The stock solution of warfarin was prepared with concentration of 20 mM. The stock solutions of other species were prepared in DMSO or pure water with concentration of 10 mM. All solution samples for spectral tests were diluted from stock solutions to proposed concentrations and mixed in sample bottles on a vortexer (2500 rpm) for 1 min.

2.2 Urine sample

Urine samples were voluntarily provided by the first author in this work who signed informed consent forms prior to collection, in accordance with the ethical research guidelines of our institution. All experiments involving the collected samples were conducted in compliance with relevant laws and institutional guidelines. The study strictly adhered to the general principles outlined in the Declaration of Helsinki. Urine samples were stored at -20 °C and used within 24 h. 2 μL of the DCTB stock solution was mixed with 0.2 mL urine sample and 1.8 mL PBS buffer spiked of HSA. All urine samples were vigorously vortexed for 1 min before recording on fluorometer.

2.3 Molecular docking

The 3D geometry of ligand (DCTB) was minimized by a mm2 job in Chem3D. The ligand-free crystal structure of albumin (PDB ID: 4K2C) was taken from the Brookhaven Protein Data Bank (http://www.rcsb.org/pdb). Flexible ligand docking was performed by AutoDock 4.2 molecular docking program using the implemented empirical free energy function and the Lamarckian Genetic Algorithm. The Autogrid was used to calculate Grids. The grid spacing was 0.375 Å as default. 20 docking runs

with 2,500,000 energy evaluations were performed. Binding energy of each complex was recorded directly from AutoDock. The output from AutoDock was rendered with PyMol. The 2D diagrams were produced by a ligplus software.

2.4 The Lippert-Mataga equation [1, 2]

$$\Delta\nu = \frac{2(\mu_g - \mu_e)^2}{hca_0^3}\Delta f + C \quad (1)$$

$$\Delta f = \frac{\varepsilon - 1}{2\varepsilon + 1} - \frac{n^2 - 1}{2n^2 + 1} \quad (2)$$

$$a_0 = \left(\frac{3M}{4N\pi d}\right)^{\frac{1}{3}} \quad (3)$$

where $\Delta\nu$ is the Stokes shift (cm^{-1}) between the absorption and fluorescence emission peak, h is the Planck constant, c is the velocity of light in vacuum, $\Delta\mu$ is the transition dipole moments between the ground (μ_g) and excited (μ_e) states, Δf is the orientation polarizability of the solvents expressed by the dielectric constant (ε) and refractive index (n) of the solvents and a_0 is the Onsager cavity radius, which can be derived from the Avogadro number N, molecular weight M, and density d (d = 1.0 g/cm^3).

2.5 Calculation of binding constant (K_b) and stoichiometry (n)

The binding parameters can be calculated using fluorescence data. The calculation of binding constant (K_b) and binding stoichiometry (n) can be conducted based on the previously reported equations [3].

$$\log\left(\frac{F_0 - F}{F}\right) = \log K_b + n \log [Q] \quad (4)$$

2.6 Limit of detection

The limit of detection (LOD) for HSA was calculated by using $3\sigma/\kappa$ rule based on HSA titration experiments. Where σ is the standard deviation of blank measurement for ten times and κ is the slope of the fluorescent intensity plotted against the HSA

concentration.

2.7 The miniaturized testing system

The portable miniaturized testing system was fabricated using polyamide fiber by 3D printing. This system was composed by a holder to fix the UV flashlight (365 nm), a sample holder to place the quartz cell (1 × 1 cm), and a smartphone for the photo capture (iphone13). The quartz cell was added with 2 mL of DCTB (10 μM) in PBS (1 mM, pH 7.4) as the working solution. The testing samples containing different concentrations of HSA were added into the working solution and were vigorously vortexed for 10 s before capturing. Finally, the fluorescence of quartz cell was captured and analyzed by Photoshop application on computer.

2.8 Fluorescence lifetime

Fluorescent decay curves were recorded by a Horiba Delta-Flex instrument with a NanoLED with peak wavelength at 453 nm (pulse duration < 1.4 ns). Lifetime was recorded at peak wavelength. IRF is the instrument response function (prompt). The radiation decay curves were typically fit to the multi-exponential model: $I(t) = A + I_0 \sum \alpha_i \exp(-t/\tau_i)$. The I_0 represents the original fluorescent intensity; the α_i are pre-exponential factors, which represent the fractional amount of each lifetime component and the $\sum \alpha_i$ isormalized to unity; the τ_i refers to fluorescence lifetimes. The average fluorescence lifetime is calculated by equation: $\tau = \sum \alpha_i \tau_i$.

3. Synthesis

3.1 Synthesis of DCTB

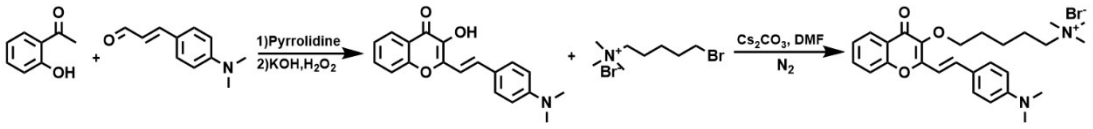

DCTB can be easily obtained through a two-step reaction, as illustrated in above graph. The intermediate HSF was synthesized following our previously reported method [4]. HSF (0.4605 g, 1.5 mmol), 5-Bromo-N,N,N-trimethylpentane-1-aminium bromide (0.867 g, 3 mmol) and Cs_2CO_3 (0.975 g, 3 mmol) were dissolved in 15 ml dry DMF and the mixture was stirred at 75 ℃ under N_2 atmosphere for 24 h. The solution was poured into iced water and extracted by ethyl acetate. The organic phase was washed by $NaHCO_3$ solution and concentrated under vacuum conditions. The crude product was purified by column chromatography with a mixed solution of methanol and dichloromethane (1 / 10, v / v) to obtain a red solid (0.32 g, yields: 41.5 %). ^{1}H NMR (500 MHz, DMSO-d_6): δ = 8.10 – 8.00 (m, 1H), 7.81 – 6.39 (m, 9H), 4.15 – 4.02 (m, 2H), 3.32 – 2.68 (m, 17H), 1.85 – 1.72 (m, 4H), 1.48 (dp, J = 23.0, 7.8 Hz, 2H). ^{13}C NMR (126 MHz, DMSO-d_6): δ = 173.34, 156.37, 154.74, 151.89, 151.06, 139.24, 138.14, 137.39, 134.43, 132.02, 129.91, 125.37, 124.41, 123.21, 118.34, 112.55, 111.55, 109.77, 72.55, 65.78, 52.67, 29.39, 22.99, 22.31. HRMS: m/z: calcd. for [M] ([$C_{27}H_{35}N_2O_3$]): 435.26; found: 435.26.

3.2 Synthesis of DHC

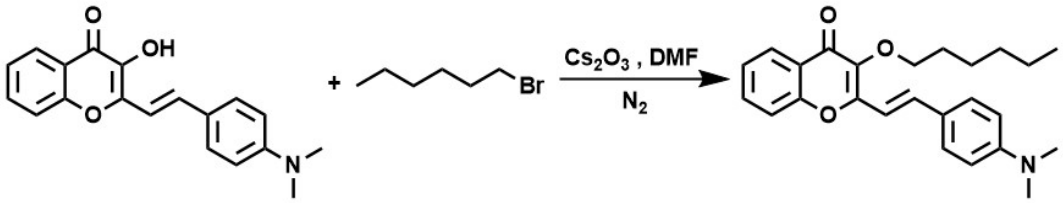

HSF (0.4605 g, 1.5 mmol), bromohexane (0.495 g, 3 mmol) and Cs_2CO_3 (0.975 g, 3 mmol) were dissolved in 15 ml dry DMF and the mixture was stirred at 70 ℃ under N_2 atmosphere for 24 h. The solution was poured into iced water and extracted by ethyl acetate. The organic phase was washed by $NaHCO_3$ solution and concentrated under vacuum conditions. The crude product was purified

by column chromatography with a mixed solution of ethyl acetate and petroleum ether (1 / 3, v / v) to obtain a red solid (0.12 g, yields: 20.5 %). ^{1}H NMR (500 MHz, DMSO-d_6): δ = 8.05 (ddd, J = 7.9, 6.1, 1.7 Hz, 1H), 7.82 – 6.38 (m, 9H), 4.11 – 4.04 (m, 2H), 2.99 (d, J = 17.9 Hz, 6H), 1.70 (dt, J = 30.5, 7.6 Hz, 2H), 1.45 (d, J = 37.7 Hz, 2H), 1.36 – 1.28 (m, 4H), 0.88 (q, J = 7.2 Hz, 3H). ^{13}C NMR (126 MHz, DMSO-d_6): δ = 172.99, 156.23, 154.71, 151.82, 138.18, 137.13, 134.06, 129.74, 125.37, 125.07, 124.43, 123.23, 118.41, 112.50, 109.83, 72.90, 31.55, 29.90, 25.83, 22.54, 14.41. HRMS: m/z: calcd. for $[M + H]^+$ ($[C_{25}H_{29}NO_3] + H)^+$: 392.21; found: 392.20.

4. Figures and Tables

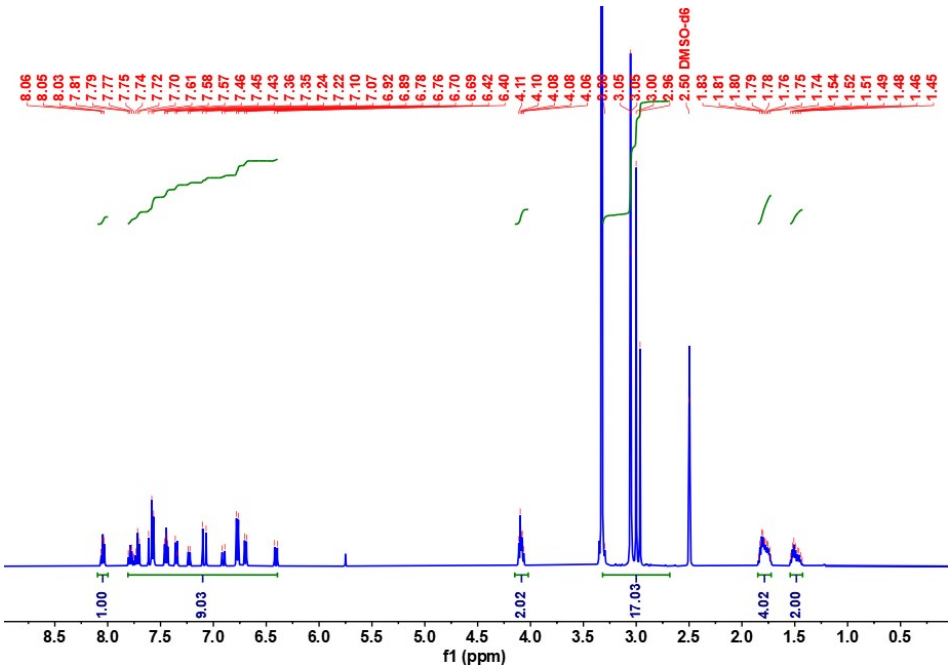

Fig. S1 ^{1}H NMR spectrum of DCTB in DMSO-d_6

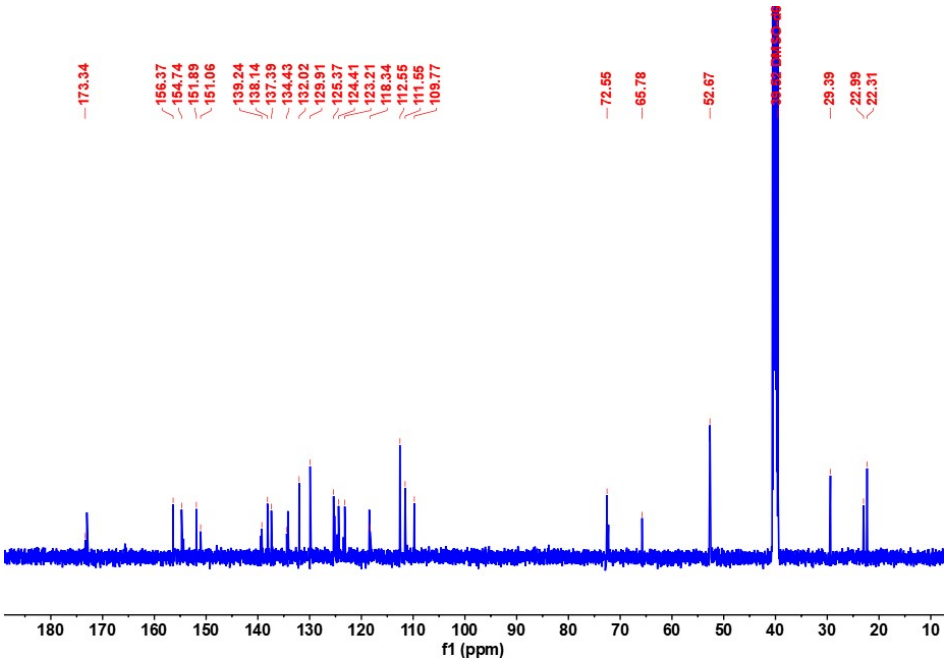

Fig. S2 ^{13}C NMR spectrum of DCTB in DMSO-d_6

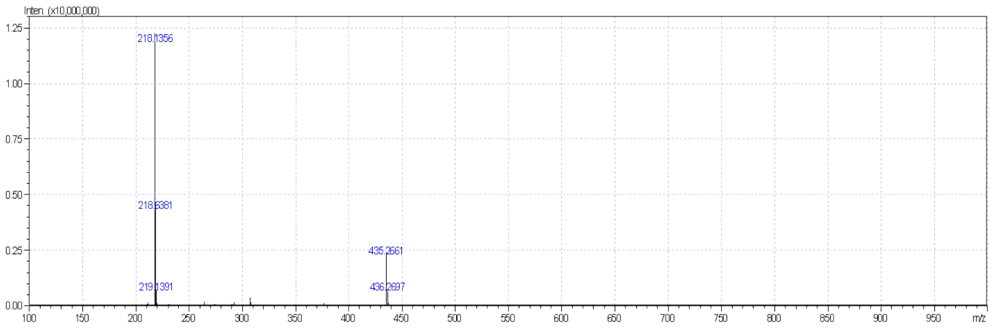

Fig. S3 HRMS spectrum of DCTB

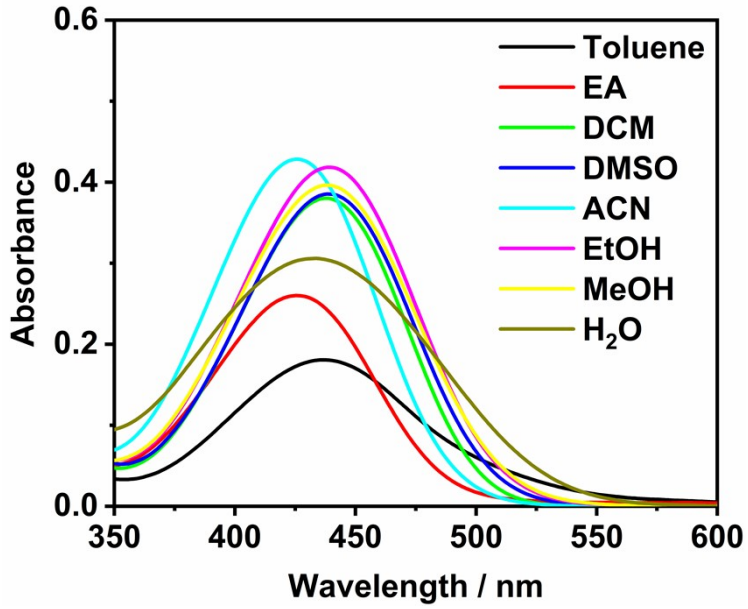

Fig. S4 Absorption spectra of DCTB in different solvents. [DCTB] = 10 μM.

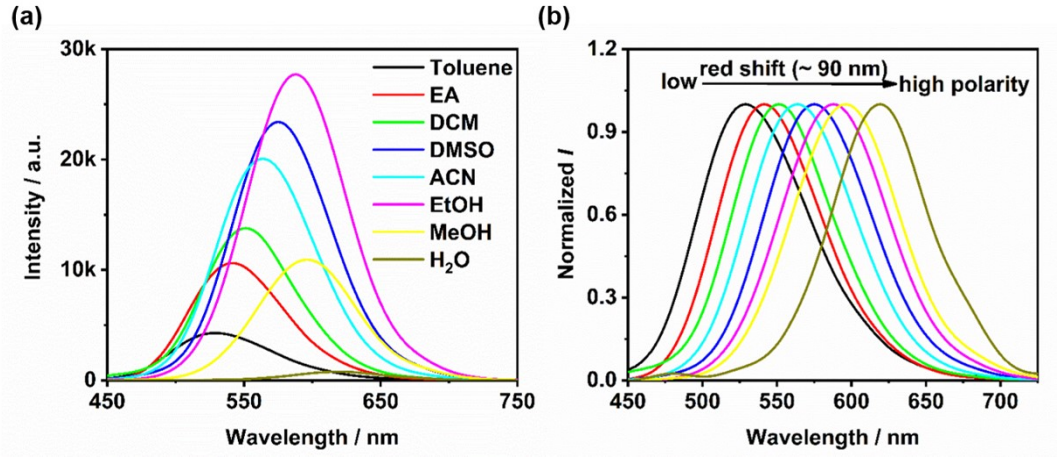

Fig. S5 Fluorescence and normalized fluorescence spectra of DCTB in different solvents. [DCTB] = 10 μM. λ_{ex} = 440 nm.

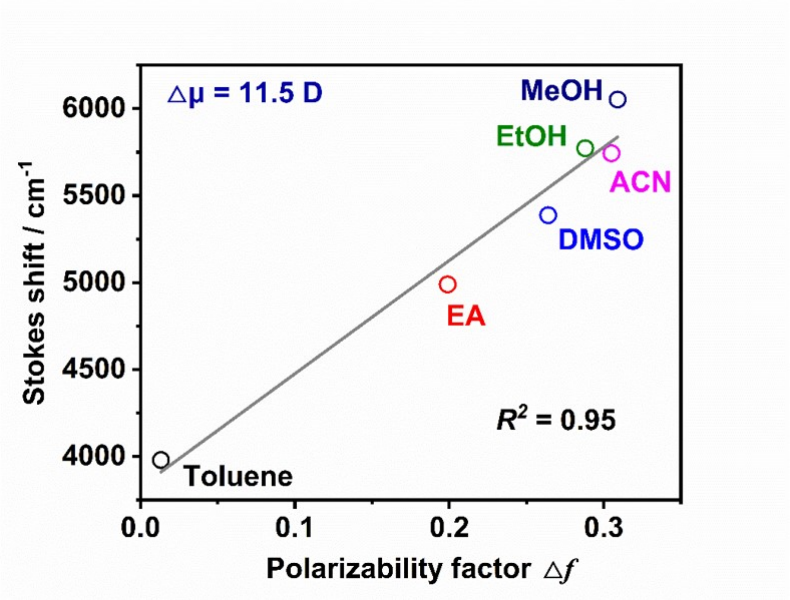

Fig. S6 Lippert-Mataga plot of DCTB. [DCTB] = 10 μM. λ_{ex} = 440 nm.

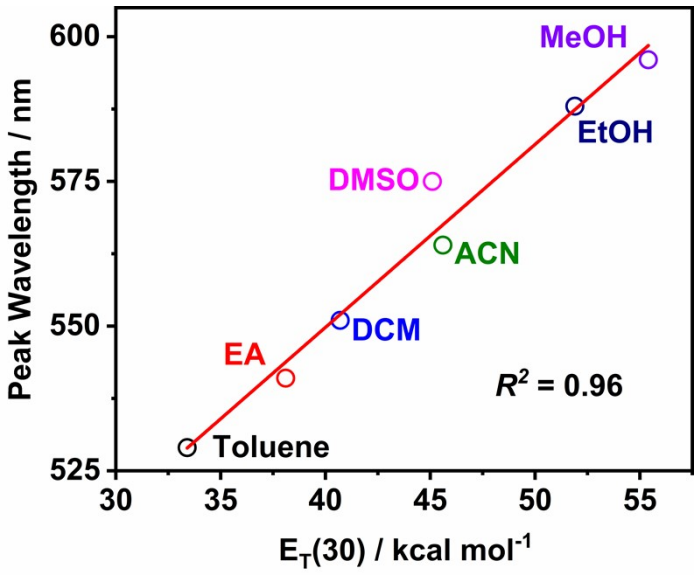

Fig. S7 The dependence of peak wavelength on polarity parameter $E_T(30)$ of different solvents. [DCTB] = 10 μM. λ_{ex} = 440 nm.

Table S1 The photophysical properties of DCTB in different solvents.

Solvents	Polarizability factor Δf	$E_T(30)$ (kcal/mol) [a]	Abs (nm) [b]	ε ($\times 10^4$ $M^{-1}cm^{-1}$) [c]	E_m (nm) [d]	Stokes shift (cm^{-1}) [e]
Toluene	0.013	33.4	437	0.136	529	3979
EA	0.199	38.1	426	0.125	541	4989
DMSO	0.263	45.1	439	0.130	575	5387
ACN	0.305	45.6	426	0.146	564	5743
EtOH	0.288	51.9	439	0.100	588	5772
MeOH	0.309	55.4	438	0.145	596	6052

Note: [a] $E_T(30)$ is empirical polarity parameter. Δf is the polarizability factor in Lippert-Mataga equation. [b] Abs and [d] E_m represent emission of the peak wavelengths of ultraviolet and fluorescence of the dye in different solvents, respectively. [c] ε is molar extinction coefficient. [e] Stokes shift is calculated based on Abs and E_m.

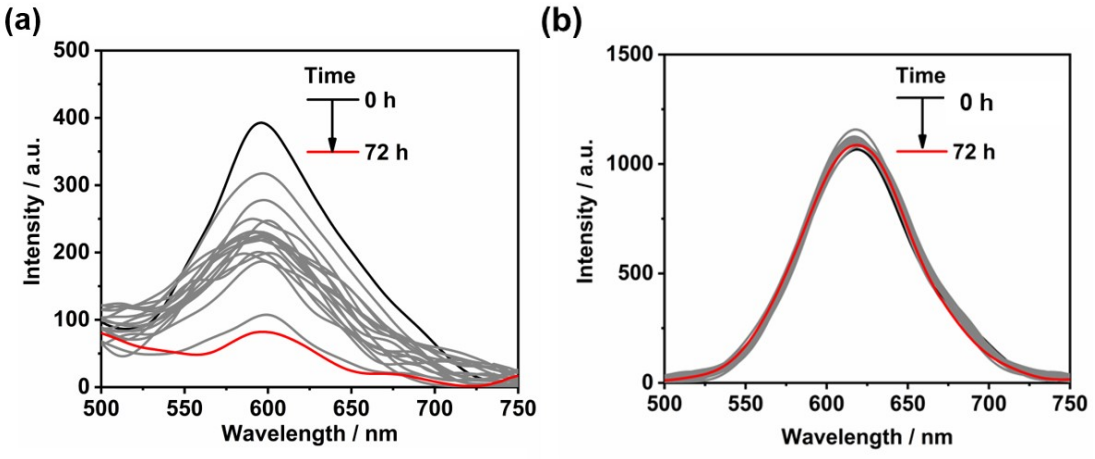

Fig. S8 Time-dependent intensity changes of (a) 4MC and (b) DCTB. [4MC] = [DCTB] = 10 μM. λ_{ex} = 440 nm.

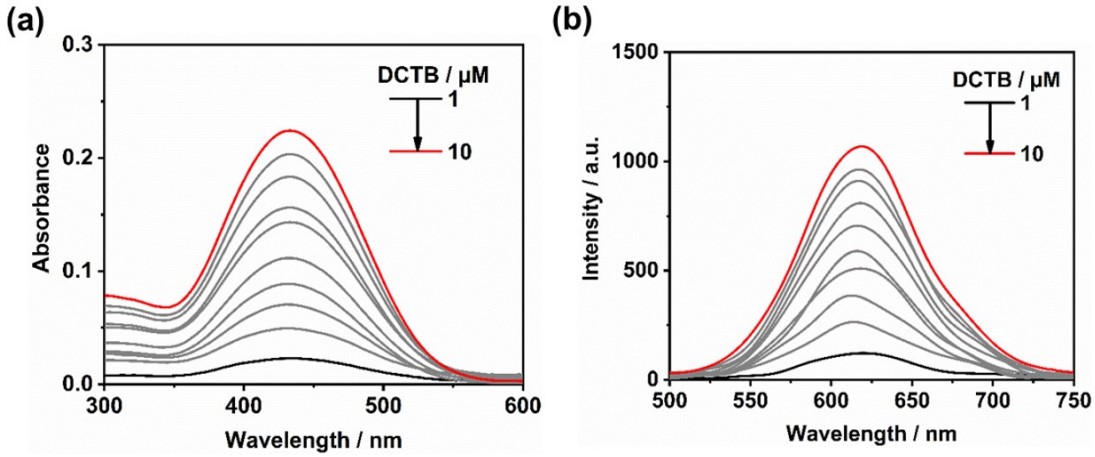

Fig. S9 (a) Absorption spectra and (b) fluorescence spectra of DCTB with different concentrations (1-10 μM) in PBS.

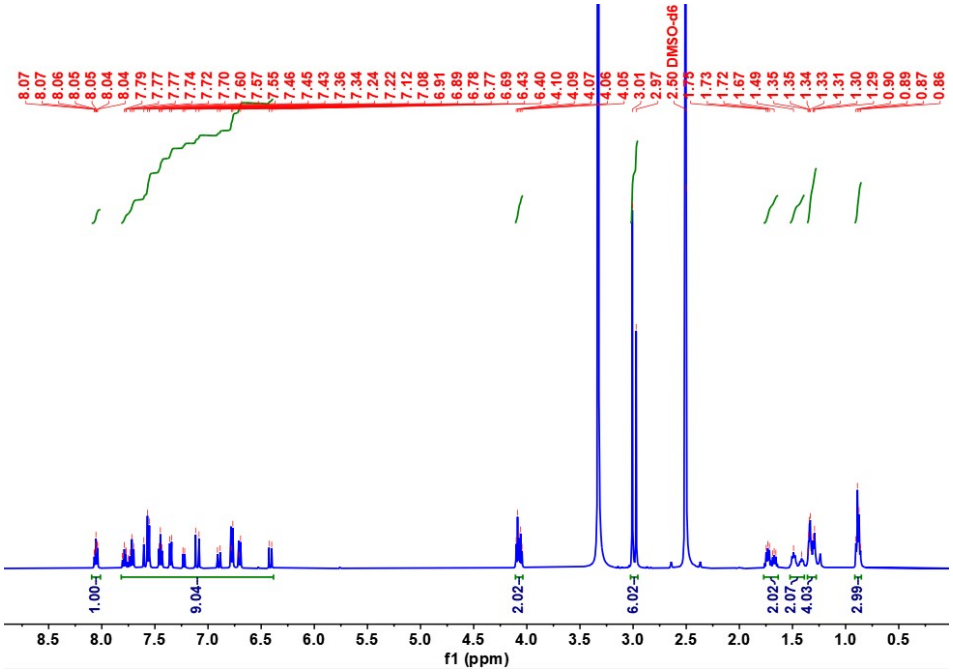

Fig. S10 ^{1}H NMR spectrum of DHC in DMSO-d_6

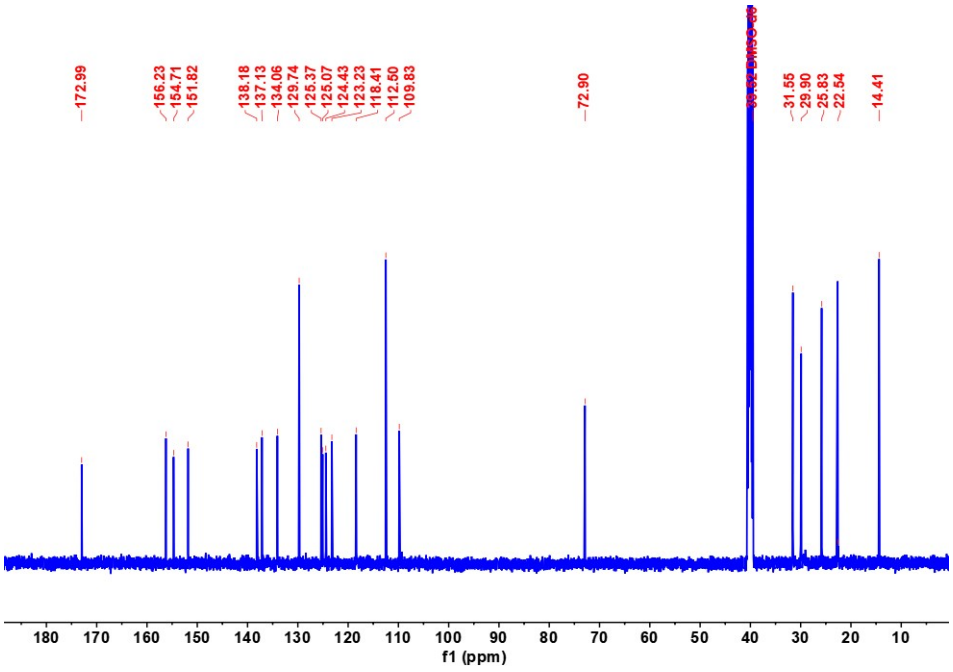

Fig. S11 ^{13}C NMR spectrum of DHC in DMSO-d_6

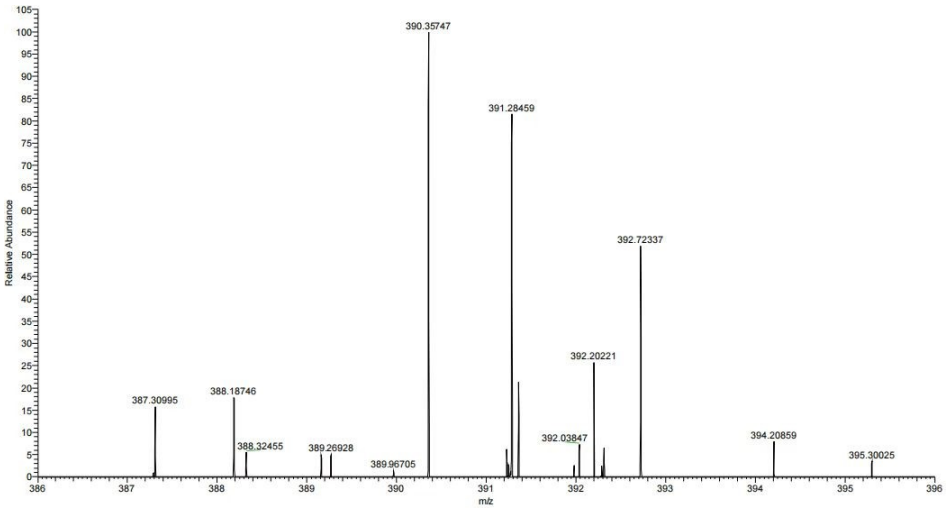

Fig. S12 HRMS spectrum of DHC

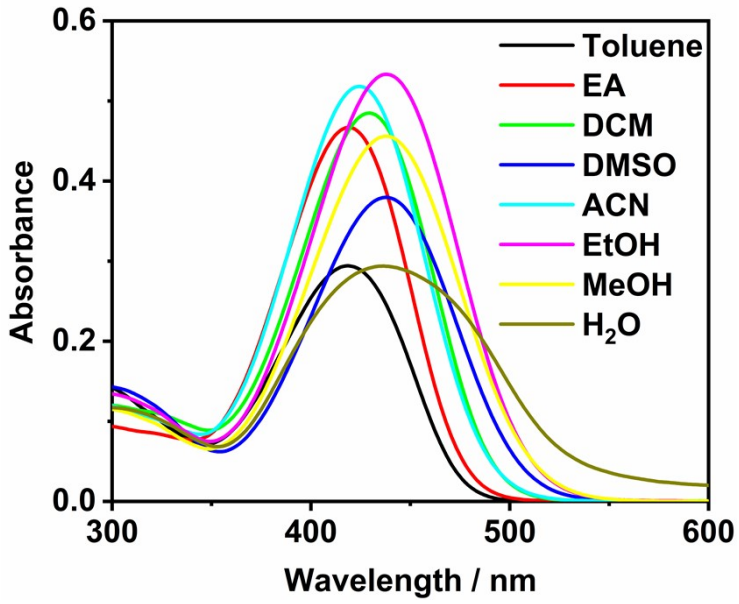

Fig. S13 Absorption spectra of DHC in different solvents. [DHC] = 10 μM.

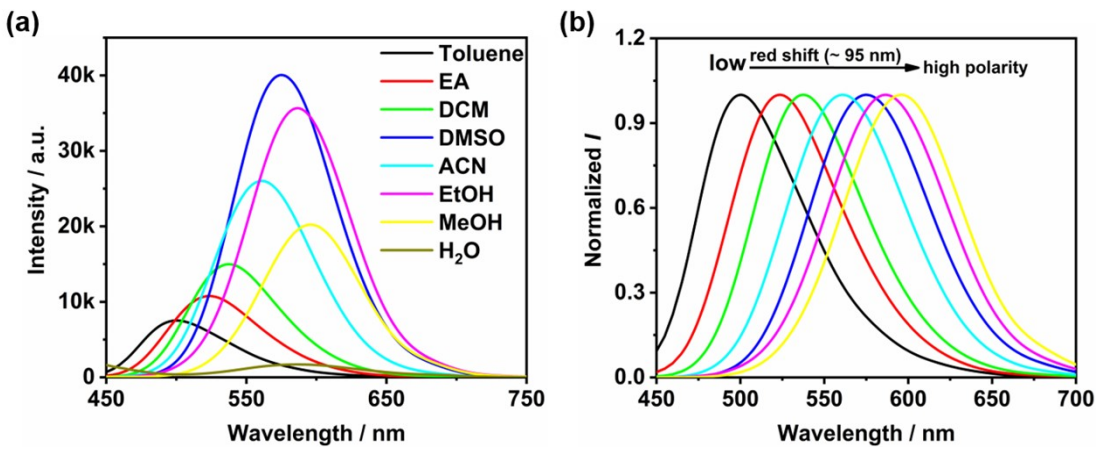

Fig. S14 (a) Fluorescence and (b) normalized fluorescence spectra of DHC in different solvents. [DHC] = 10 μM. λ_{ex} = 440 nm.

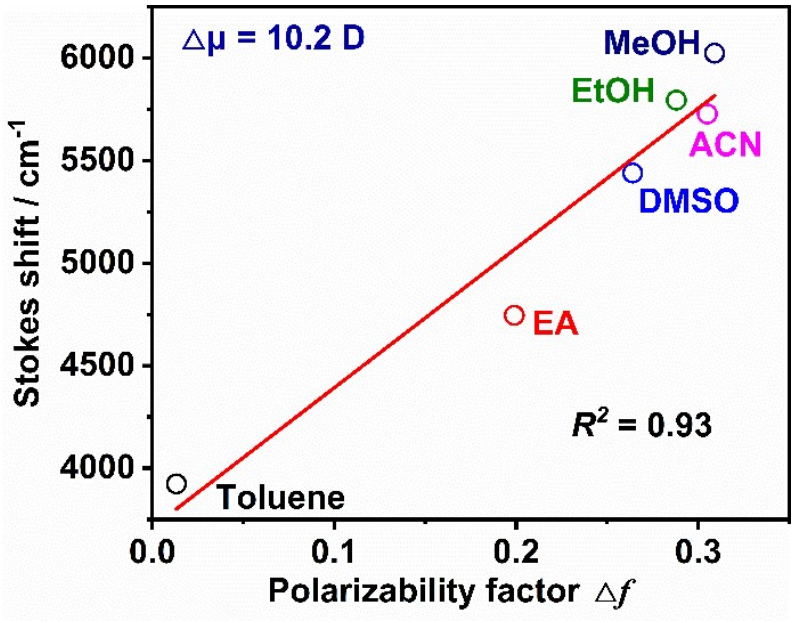

Fig. S15 Lippert-Mataga plot of DHC. [DHC] = 10 μM. λ_{ex} = 440 nm.

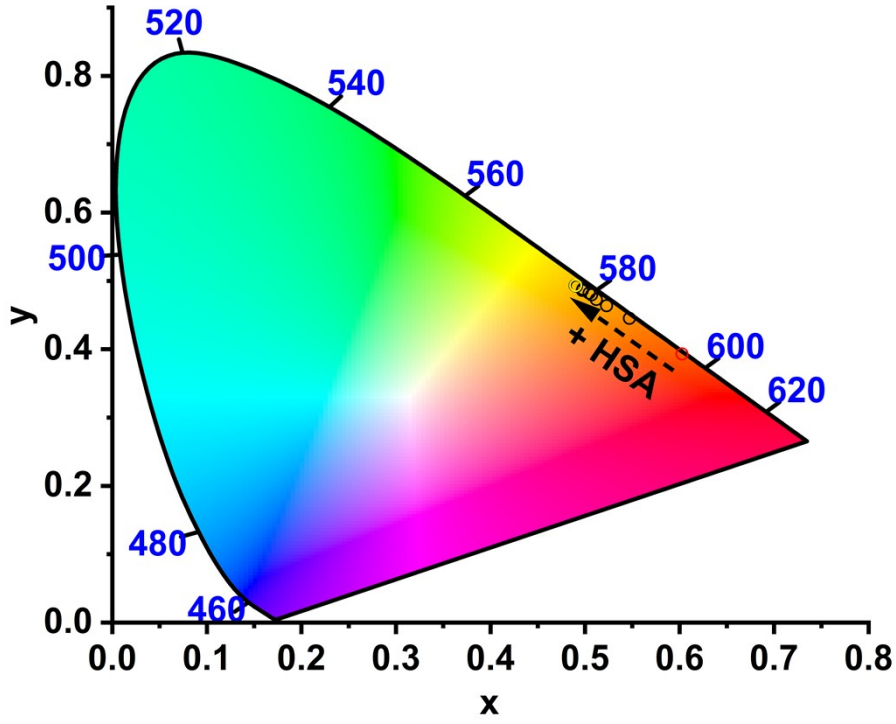

Fig. S16 Fluorescence changes in the CIE diagram of DCTB (10 μM) with the increase of HSA in PBS (λ_{ex} = 440 nm).

Fig. S17 3D-printed testing device.

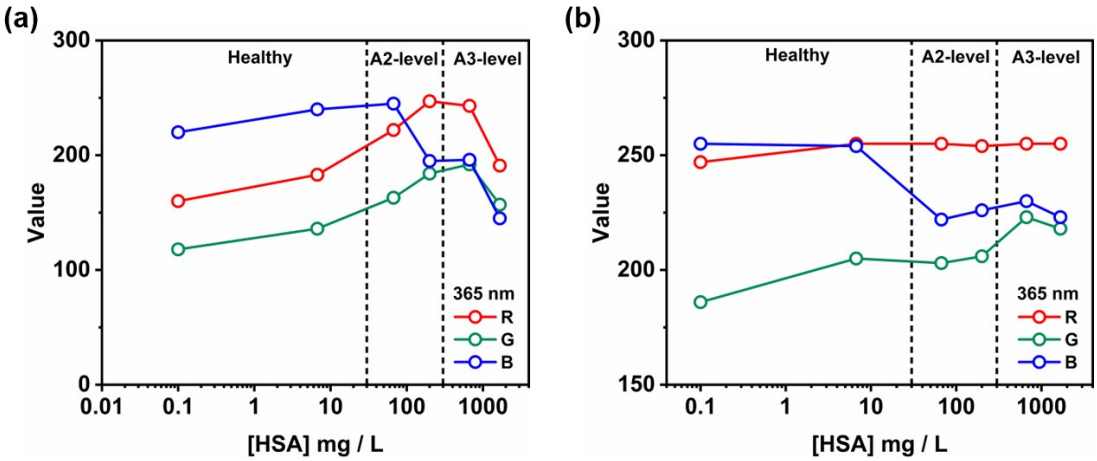

Fig. S18 The RGB values in (a) black box and (b) 3D-printed testing device.

5. References

[1] N.A. Sayresmith, A. Saminathan, J.K. Sailer, S.M. Patberg, K. Sandor, Y. Krishnan, M.G. Walter, Photostable Voltage-Sensitive Dyes Based on Simple, Solvatofluorochromic, Asymmetric Thiazolothiazoles, Journal of the American Chemical Society, 141 (2019) 18780-18790.

[2] T. Qin, B. Liu, B. Du, Y. Huang, G. Yao, Z. Xun, H. Xu, C. Zhao, Solvatofluorochromic flavonoid dyes with enlarged transition dipole moments enable the ratiometric detection of methanol in commercial biodiesel with improved sensitivities, Journal of Materials Chemistry C, 8 (2020) 16808-16814.

[3] S. Hadidi, A binuclear Cu(I)-phosphine complex as a specific HSA site I binder: synthesis, X-ray structure determination, and a comprehensive HSA interaction analysis, Journal of Biomolecular Structure and Dynamics, 41 (2022) 7616-7626.

[4] T. Qin, X. Zhao, C. Song, T. Lv, S. Chen, Z. Xun, Z. Xu, Z. Zhang, H. Xu, C. Zhao, B. Liu, X. Peng, A ratiometric supramolecular fluorescent probe for on-site determination of cyfluthrin in real food samples, Chem. Eng. J. 451 (2023) 139022.